Interstellar dehydrogenated PAH anions: vibrational spectra

Mridusmita Buragohain,[1] Amit Pathak,[2]* Peter Sarre[3] and Nand Kishor Gour[4]

[1]*Department of Physics, Tezpur University, Tezpur 784028, India*
[2]*Department of Physics, Banaras Hindu University, Varanasi 221 005, India*
[3]*School of Chemistry, The University of Nottingham, University Park, Nottingham NG7 2RD, UK*
[4]*Department of Chemical Sciences, Tezpur University, Tezpur 784 028, India*

ABSTRACT
Interstellar polycyclic aromatic hydrocarbon (PAH) molecules exist in diverse forms depending on the local physical environment. Formation of ionized PAHs (anions and cations) is favourable in the extreme conditions of the interstellar medium (ISM). Besides in their pure form, PAHs are also likely to exist in substituted forms; for example, PAHs with functional groups, dehydrogenated PAHs etc. A dehydrogenated PAH molecule might subsequently form fullerenes in the ISM as a result of ongoing chemical processes. This work presents a density functional theory (DFT) calculation on dehydrogenated PAH anions to explore the infrared emission spectra of these molecules and discuss any possible contribution towards observed IR features in the ISM. The results suggest that dehydrogenated PAH anions might be significantly contributing to the 3.3 μm region. Spectroscopic features unique to dehydrogenated PAH anions are highlighted that may be used for their possible identification in the ISM. A comparison has also been made to see the size effect on spectra of these PAHs.

Key words: astrochemistry – molecular processes – ISM: lines and bands – ISM: molecules.

1 INTRODUCTION

Mid-infrared emission lines popularly known as 'aromatic infrared bands' (AIBs) are broad emission features widely distributed in the interstellar medium (ISM) and observed at 3.3, 6.2, 7.7, 8.6, 11.2, 12.7 and 16.4 μm towards diverse astrophysical objects (Tielens 2008). The regions where the AIBs are observed include H II regions, reflection nebulae, planetary nebulae, photodissociation regions, asymptotic giant branch objects, active star forming regions, young stellar objects, the diffuse interstellar medium, external galaxies, etc. (Onaka et al. 1996; Verstraete et al. 1996; Hony et al. 2001; Peeters et al. 2002; Acke & van den Ancker 2004; Regan et al. 2004; Sakon et al. 2004; Brandl et al. 2006; Armus et al. 2007). Lately, AIBs have emerged as an acclaimed area of research due to their numerous detections in the ISM and the ambiguity associated in the identification of their carriers. It was first proposed by Duley & Williams (1981) that these features arise from the thermal emission by small carbon grains with functional groups. This hypothesis was later revised by Léger & Puget (1984) and Allamandola, Tielens & Barker (1985) to free, gas-phase polycyclic aromatic hydrocarbon (PAH) molecules, giving rise to these features in the mid-IR as a result of vibrational relaxation on absorption of background UV photons. The PAH-AIB hypothesis is now widely accepted, though uncertainty lies in the identification of the exact form and

functional groups attached to the PAH molecule. An increasing number of observations point to a wide range of PAHs rather than a single conventional form which may explain the complete set of AIBs (Snow et al. 1998; Peeters et al. 2004; Hudgins et al. 2005; Simon et al. 2011; Onaka et al. 2014; Buragohain et al. 2015). A recent study by Yang et al. (2017a) has proposed interstellar PAH molecules to be a mixture of aromatic/aliphatic components.

PAH molecules have also been suggested to be potential candidates for producing absorption features in the optical region known as 'diffuse interstellar bands (DIBs)' (Cox et al. 2006; Sarre 2006; Pathak & Sarre 2008; Salama et al. 2011) and may be contributing significantly to other important interstellar phenomena, e.g. heating of the ISM and charge balance inside molecular clouds (Lepp & Dalgarno 1988b; Verstraete et al. 1990; Bakes & Tielens 1994; Bakes et al. 2001a; Bakes et al. 2001b).

The AIBs vary in terms of peak position, band width and intensity as a function of the local physical condition of the observed sources (Hony et al. 2001; Peeters et al. 2002; Tielens 2008). An overall correlation among the bands is consistent across the source environment. It is concluded that neutral, cationic as well as anionic PAHs contribute to the emission of some infrared bands depending on the interstellar conditions (Bauschlicher et al. 2008, 2009). Emission at 6.2, 7.7 and 8.6 μm is mostly contributed by PAH cations whereas the 3.3 and 11.2 μm bands preferentially arise from neutral PAHs in the ISM (Peeters et al. 2002; Tielens 2008; Schmidt, Pino & Bréchignac 2009). Cationic PAHs show a comparatively weaker 3.3 μm compared to neutrals. PAH cations are abundant in intense

* E-mail: ms.mridusmita@gmail.com (MB); amitpah@gmail.com (AP)

UV irradiated fields where PAHs are predominantly affected by photoionization (Omont 1986). In contrast to this, a comparatively less intense UV irradiated field can leave a PAH negatively charged, or an anion formed by addition of an electron (Omont 1986). Observational evidence for negatively charged molecules in the dense molecular cloud TMC-1 adds strength to the probable existence of astrophysical PAH anions (McCarthy et al. 2006). Several theoretical and experimental studies (Lepp & Dalgarno 1988a; Szczepanski, Wehlburg & Vala 1995; Bakes, Tielens & Bauschlicher 2001a; Bakes et al. 2001b; Ruiterkamp et al. 2002; Malloci et al. 2005; Wang et al. 2005; Malloci, Joblin & Mulas 2007) discuss the role of astrophysical PAH anions heating the ISM, free electron density, recombination processes, etc. Herbst (1981) and Herbst & Osamura (2008) showed that negative ions are formed through radiative attachment of electrons to neutral species in dense clouds. In a similar way, PAHs can bear a significant fraction of the negative charge which then become the principal carriers of the negative charge in the cold interstellar medium. When an electron is attached to a PAH molecule, the resultant can be a transient negative ion $[PAH_n^-]^*$ which further can decay into a stable full anion PAH_n^- or to a dehydrogenated PAH anion (PAH_{n-1}^-) through subsequent loss of an H atom (Garcia-Sanz et al. 2013). Besides, dehydrogenated PAH molecules have larger electron affinities compared to the parent hydrocarbons which indicates a significant presence of dehydrogenated PAH anions in environments like diffuse or circumstellar media (Hammonds et al. 2011). Tobita et al. (1992) showed the formation of a dehydrogenated PAH anion from a PAH molecule and reported that dehydrogenated PAH anions are the only possible fragment anions formed. Thus, any astrophysical model that takes account of interstellar PAH anions should also include dehydrogenated forms. The dehydrogenation state of PAH molecules in the ISM is further endorsed by the recent detection of fullerenes as carriers for two observed DIBs (Campbell et al. 2015; Ehrenfreund & Foing 2015). It is proposed that cosmic fullerenes may be formed from interstellar PAHs in a top-down or a bottom-up process (Berné & Tielens 2012; Dunk et al. 2012). In either of the two formation processes initiated by PAHs, dehydrogenated PAHs are an intermediate form (Mackie et al. 2015) which may subsequently be altered into other forms; for example, a dehydrogenated PAH anion through radiative attachment of electrons in dense cloud.

This work reports a density functional theory (DFT) of PAH anions (PAH_n^-) along with dehydrogenated forms (PAH_{n-1}^-) to study their possible spectral characteristics in the infrared in relation to the AIBs. PAH anions are astrophysically important as these have more stable configuration (in terms of energy) compared to cations and neutrals under interstellar conditions. The size effect on the intensity of vibrational transitions of these PAHs is also studied in this report.

2 THEORETICAL APPROACH

Compared to laboratory experiments, theoretical quantum chemical calculations have appeared to be more feasible to study the chemical and physical properties of PAH molecules. DFT is an appropriate quantum chemical method that has been used rigorously to calculate the vibrational properties of interstellar molecules in order to compare with the observed AIBs (Langhoff 1996; Hudgins, Bauschlicher & Sandford 2004; Pathak & Rastogi 2005, 2006, 2007; Pauzat 2011; Pauzat et al. 2011; Candian, Sarre & Tielens 2014). DFT can be applied on a wide range of PAH molecules of varying size, charge and functional groups including molecules that are not easily synthesized in the laboratory. An appropriate com-

bination of basis set and functional is chosen to compromise between accuracy of the results and computational demand (Yang et al. 2017a). For the present study, we are performing DFT combined with B3LYP/6-311G** basis on PAH molecules to calculate the optimized structure of the molecules which is further used to obtain the harmonic frequencies and intensities of vibrational modes at the same level of theory. Vibrational modes in a PAH molecule are of different types, for example: $C–H_{oop}$ (out of plane), $C–H_{inplane}$, $C–C_{stretch}$ and $C–H_{stretch}$. The frequencies obtained from the results of quantum chemical calculation are overestimated as compared to the experimental data. In order to match with the experimental frequencies, computed frequencies are scaled down with mode-dependent scaling factors. A scaling factor of 0.974 for $C–H_{oop}$, 0.972 for $C–H_{inplane}$ and $C–C_{stretch}$ and 0.965 for $C–H_{stretch}$ is used (Buragohain et al. 2015, 2016). These scaling factors are calculated by comparing experimental and theoretical frequencies. When the relative strengths of the modes obtained from theoretical calculation are compared with those obtained from experiments, the intensity of C–H stretch is found to be much larger as compared to the other modes and an intensity scaling is required. Considering that the second-order Møller–Plesset (MP2) perturbation theory with large basis set (for example, MP2/6-311+G(3df, 3pd)) gives more accurate oscillator strengths compared to B3LYP DFT, Yang et al. (2017b) have derived a relation for MP2/6-311+G(3df, 3pd) and B3LYP/6-311+G** level of theories to scale the intensities of $C–H_{stretch}$ modes near ∼3 μm region. There are two important features in this region; 3.3 and 3.4 μm due to the stretching of aromatic C–H and aliphatic C–H bonds, respectively. By using, $A_i \approx 0.6372 A_j$, where A_i and A_j are the intensities of $C–H_{stretch}$ modes computed at the MP2/6-311+G(3df, 3pd) and B3LYP/6-311+G** level, respectively, we can achieve good accuracy by computing at an inexpensive level (Yang et al. 2017b). Relative intensities (Int_{rel}[1]) are obtained by taking the ratio of all intensities to the maximum intensity for normalization. The computed position (in wavelength) and relative intensity (Int_{rel}) of the lines are used to plot a Gaussian profile with a full width at half-maximum of $30\,cm^{-1}$. The profile width is typical for PAHs emitting in an interstellar environment and depends on vibrational energy redistribution of the molecule (Allamandola, Tielens & Barker 1989). In some cases, a few overlapping bands in a particular region (mostly in the 3 μm region) might add up producing band intensities to exceed unity in the resulting spectra (Buragohain et al. 2015, 2016). It is important to note here that for some species, several (at least 2) spin-multiplicities are possible (for $C_{24}H_{11}^-$ for instance, singlet and triplet spin states are a priori possible). However, as a preliminary study, we have limited our calculation to molecules with the lowest possible spin-multiplicity. This is because the sample molecules that we have considered exhibit the lowest energy with the lowest possible spin-multiplicity corresponding to the most stable configuration to endure in the interstellar domain (Bauschlicher & Ricca 2013; Theis et al. 2015; Fortenberry, Moore & Lee 2016). For example, for $C_{24}H_{11}^-$, lowest lying state is a singlet state. We have used QCHEM (quantum chemistry package) to perform our calculation (Shao et al. 2015).

3 RESULTS AND DISCUSSION

Coronene ($C_{24}H_{12}$) is a mid-sized compact PAH molecule and is a good representative of the interstellar PAH family. For its sta-

---

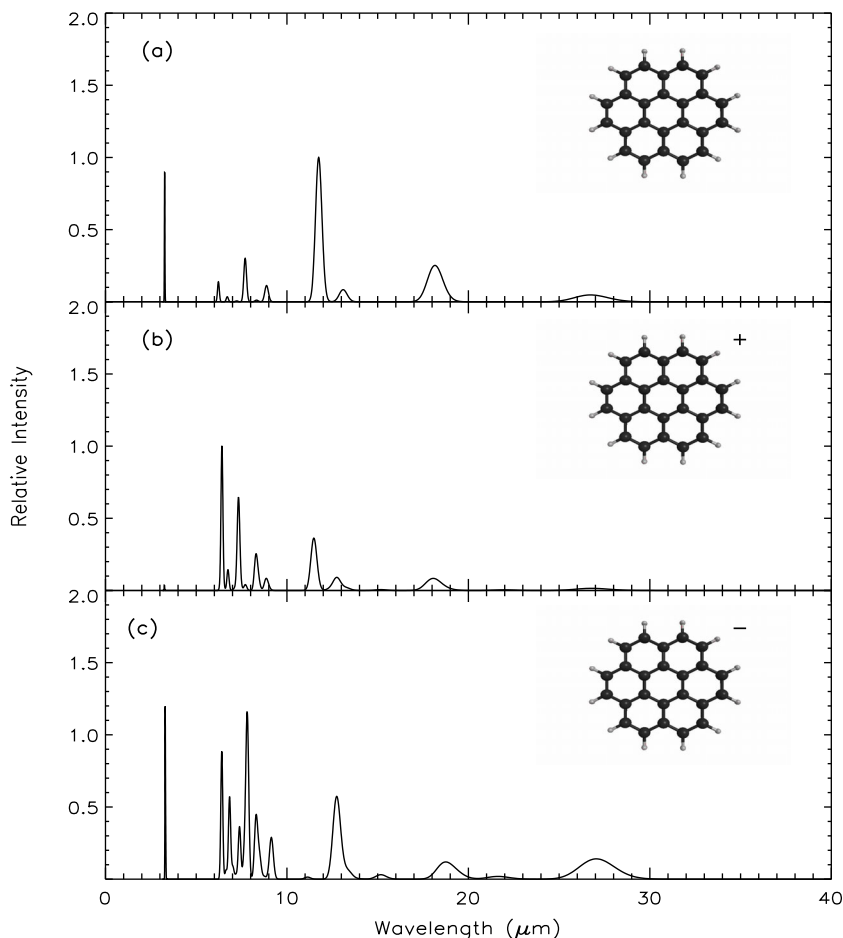[1] $Int_{rel} = \frac{absolute\ intensity}{maximum\ absolute\ intensity}$.

Figure 1. Theoretical spectra of (a) neutral coronene ($C_{24}H_{12}$), (b) cationic coronene ($C_{24}H_{12}^+$), (c) anionic coronene ($C_{24}H_{12}^-$).

ble configuration due to the delocalization of the electrons and its compactness, coronene is considered as a good choice for our study. We compare the IR spectra of neutral coronene ($C_{24}H_{12}$) with its cationic ($C_{24}H_{12}^+$) and anionic ($C_{24}H_{12}^-$) forms in Fig. 1. The features are characteristic of various vibrational modes present in the respective molecules. Table 1 presents the wavelengths corresponding to different modes of coronene in its neutral and ionized forms. While the wavelengths of these bands are less affected by ionization (positive or negative), a distinct variation in the intensity is produced on ionization of the molecule. This is similar to the results discussed in DeFrees et al. (1993), Langhoff (1996) and Pauzat, Talbi & Ellinger (1997). Intensities of bands in the 6–10 μm regions which are modest   in $C_{24}H_{12}$ become significantly more prominent in $C_{24}H_{12}^+$ and $C_{24}H_{12}^-$ (Figs 1b and c). The features in the 6–10 μm region are characteristic of the C–C stretch and C–H in-plane bending vibrations of the PAH molecules. The 3.3 μm feature due to the C–H stretch mode is intense for $C_{24}H_{12}$ and $C_{24}H_{12}^-$ and weak for $C_{24}H_{12}^+$. Intensities of all the 3.3 μm features are scaled here (scaling factor ∼ 0.6372). Previous laboratory and theoretical studies (Tielens 2008, and references therein) reveal that the astronomical 3.3 μm feature is likely to be dominated by the C–H stretch modes in neutral PAH molecules, whereas 5–10 μm region arises due to the C–C stretch and C–H in-plane bending modes in cationic PAH molecules. PAH anions also contribute to the 5–10 μm region and to the 3.3 μm feature which indicates them to

be an important constituent of the ISM. Importantly anionic PAHs show a comparatively strong 3.3 μm feature.

The band positions and intensities beyond 15 μm are affected to a lesser extent by ionization, both positive and negative. For example: a feature near 18 μm in neutral and cationic $C_{24}H_{12}$ which is a combination mode of C–C–C oop and C–H oop bending is shifted to 18.7 μm for anionic $C_{24}H_{12}$. Similarly, a variation in intensity is also observed, particularly a feature near 28 μm, which is a C–C–C in-plane vibration which distinctly appears in the spectrum of $C_{24}H_{12}^-$ unlike its neutral and cationic counterparts. These features in the longer wavelength side are not much studied experimentally.

Dehydrogenated forms of anions have been studied to understand any possible contribution towards the observed AIBs. Peripheral H atoms in a PAH anion molecule ($C_{24}H_{12}^-$) have been removed one-by-one to understand the effect of dehydrogenation on the spectra as shown in Fig. 2. Usually, H atoms are removed in a consecutive order, but in absence of a stable configuration, any preferable site for dehydrogenation is considered provided that the energy is minimized. As mentioned earlier, unlike neutrals all anions show rich 6−9 μm spectra which is characteristic of C–C stretch modes on the shorter wavelength side and C–H in-plane bending modes on the longer wavelength side. The intermediate is a combination of the modes. As H atoms are removed, the C–C modes gradually become dominant compared to the lesser number of C–H

Table 1. Theoretical spectral data for neutral, cationic and anionic coronene.

PAH	Frequency (cm^{-1})	Wavelength (μm)	Relative intensity	Mode
Neutral coronene	3068.32	3.3	0.43	C−H stretch
	3067.74	3.3	0.44	C−H stretch
	1607.23	6.2	0.07	C−C stretch
	1606.67	6.2	0.07	C−C stretch
	1300.34	7.7	0.15	C−C stretch + C−H in-plane
	1297.93	7.7	0.15	C−C stretch + C−H in-plane
	1127.93	8.9	0.06	C−H in-plane
	851.15	11.7	1	C−H oop bending
	550.9	18.2	0.25	C−C−C oop bending + C−H oop bending
Coronene cation	1558.29	6.4	1	C−C stretch
	1482.10	6.7	0.12	C−C stretch + C−H in-plane
	1377.30	7.3	0.1	C−C stretch + C−H in-plane
	1363.26	7.3	0.58	C−C stretch + C−H in-plane
	1206.86	8.3	0.18	C−C stretch + C−H in-plane
	1206.47	8.3	0.05	C−C stretch + C−H in-plane
	1187.09	8.4	0.07	C−H in-plane
	1130.89	8.8	0.07	C−H in-plane
	870.9	11.5	0.36	C−H oop bending
	784.04	12.8	0.09	C−C−C in-plane
	554.58	18	0.08	C−C−C oop bending + C−H oop bending
Coronene anion	3040.03	3.3	0.59	C−H stretch
	3038.47	3.3	0.57	C−H stretch
	3013.34	3.3	0.28	C−H stretch
	1563.83	6.4	0.35	C−C stretch
	1558	6.4	0.56	C−C stretch
	1505.7	6.6	0.06	C−C stretch
	1473.22	6.8	0.05	C−C stretch + C−H in-plane
	1461.75	6.8	0.54	C−C stretch +C−H in-plane
	1424.3	7	0.08	C−C stretch +C−H in-plane
	1353.75	7.4	0.36	C−C stretch +C−H in-plane
	1305.68	7.7	0.18	C−C stretch +C−H in-plane
	1286.69	7.8	0.15	C−C stretch +C−H in-plane
	1279.13	7.8	1	C−C stretch +C−H in-plane
	1206.34	8.3	0.37	C−C stretch +C−H in-plane
	1196.79	8.4	0.08	C−H in-plane
	1177.63	8.5	0.14	C−H in-plane
	1093.85	9.1	0.29	C−H in-plane
	785.14	12.7	0.48	C−H oop bending
	779.28	12.8	0.07	C−C−C stretch
	747.96	13.4	0.05	C−C−C in-plane
	535.98	18.7	0.1	C−C−C oop bending + C−H oop bending

Modes with intensity equal to or greater than 0.05 are only listed in the table.
oop is out of plane.
intensity of 3.3 μm band has been scaled.

in-plane modes and eventually for a fully dehydrogenated molecule ($N_H = 0$)[2], C–C modes are the only possible modes distributed in the 5–10 μm region. In fact, for $(C_{24}H_n)^-$ with n = 8, 6, 4, 2, 1 and 0, the C–C mode is the most intense band (Int$_{rel} \sim 1$) seen near 5.2 and 6.8 μm. The 5.2 μm band is a unique feature observed for dehydrogenated PAHs only and arises due to the stretching of those C–C bonds that are exposed on removal of its associated H atoms. The 5.2 μm band, however, does not appear immediately after dehydrogenation starts and arises only after certain dehydrogenation level is attained. In contrary to the predominance of the C–C stretch modes (5−10 μm), a distinct fall in the intensity of the 3.3 μm is found. This is obvious as the 3.3 μm feature is purely a contribution from the C–H stretch mode. For $(C_{24})^-$, this feature is absent as expected.

Besides this, the intensity of the 3.3 μm band is also affected by the symmetry of the molecule that usually is less for a more symmetric structure. When an odd number of H atoms are removed from the structure, the coronene molecule loses its symmetry by a degree lower compared to the removal of an even number of H atoms. A lower symmetry structure shows a higher intensity of the 3.3 μm feature compared to a more symmetric structure.

Usually, a coronene molecule contains duo C–H groups[3] at all sites. Removal of an odd number of H atoms from the periphery leaves one of the associated C–H units to convert into a solo

[2] N_H = number of H atoms in the periphery of a PAH molecule.

[3] A duo C–H group, also referred as doubly adjacent C–H unit, is a group with one neighbouring adjacent C–H units on the same ring.
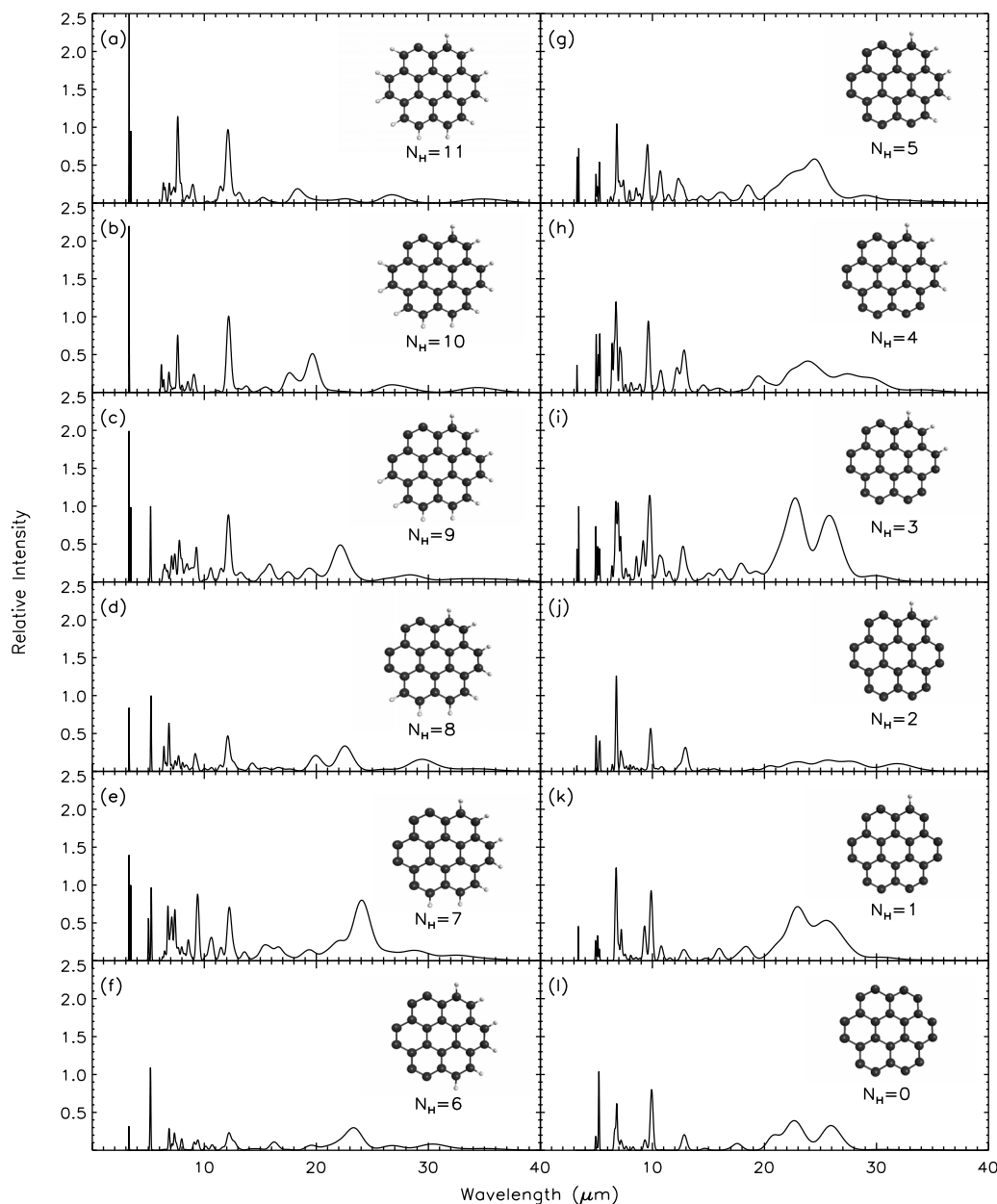
Figure 2. Theoretical spectra of (a)–(l) PAH (coronene, $C_{24}H_{12}$) anion in dehydrogenated forms.

C–H unit[4] which originally was a duo C–H group. The stretching of such a converted solo C–H produces a 3.4 μm feature. Int_{rel} values for this feature are 0.95, 0.99, 1, 0.72, 1 and 0.45, respectively, for $C_{24}H_{11}^-$, $C_{24}H_9^-$, $C_{24}H_7^-$, $C_{24}H_5^-$, $C_{24}H_3^-$ and $C_{24}H_1^-$. This is surprising as the molecules that originally have a solo C–H group do not exhibit a 3.4 μm band. The astronomical 3.4 μm feature is proposed to be originated from PAH molecules with aliphatic or superhydrogenated side groups due to the aliphatic C–H stretch (Yang et al. 2017a, and references therein).

For coronene molecules containing solo C–H groups after dehydrogenation, an oop bending mode of the solo group is present at ~11.5 μm. We suspect that these significant shifts in the bands for

a non-adjacent solo C–H unit arise due to the local electronic environment as the negative charge tends to be localized at the adjacent dehydrogenated site. As for the duo C–H groups of dehydrogenated molecules, the oop mode is redshifted and appears at ~12–13 μm. The longer wavelength features beyond 13 μm are mostly due to the C–C–C oop and C–C–C in-plane bending modes with a possible contribution from C–H oop modes in a PAH molecule. Anionic coronene ($C_{24}H_{12}^-$) shows features in the 20−30 μm region mostly due to the C–C–C in-plane modes which become significant as the dehydrogenation increases. These theoretically obtained features are unique and do not appear for any other molecule studied so far.

We also performed similar calculation for a comparatively smaller PAH–perylene ($C_{20}H_{12}$) and a comparatively larger PAH–ovalene ($C_{32}H_{14}$) to investigate any possible spectral variations. Fig. 3 shows the theoretically obtained IR spectra for a few representatives of dehydrogenated forms of $C_{20}H_{12}^-$ and $C_{32}H_{14}^-$.

---

[4] A solo C–H group, also referred as non-adjacent C–H unit, is a group with no neighbouring adjacent C–H units on the same ring.
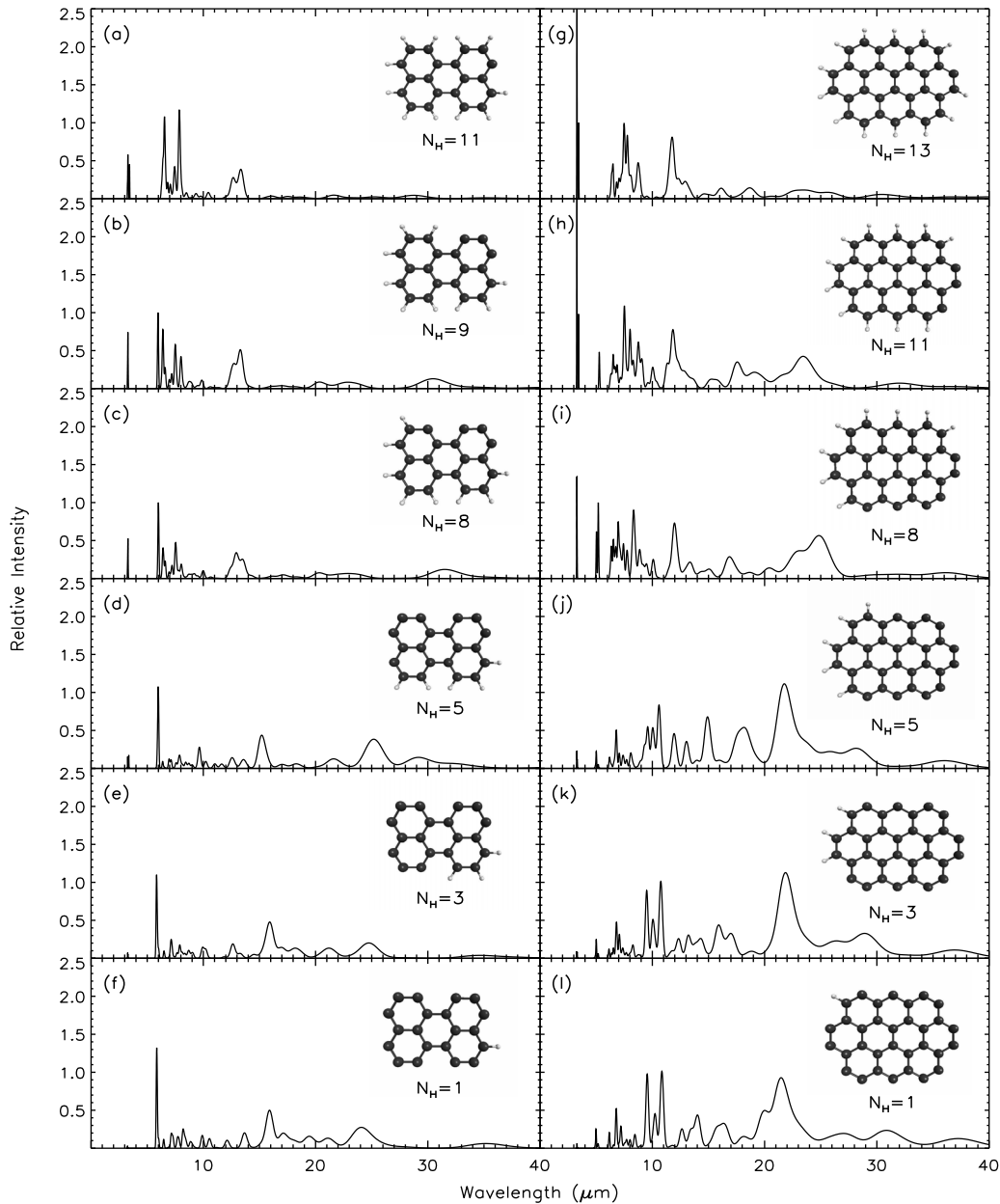
Figure 3. Theoretical spectra of randomly selected dehydrogenated forms of (a)–(f) perylene anion ($C_{20}H_{12}^-$), (g)–(l) ovalene anion ($C_{32}H_{14}^1$) anion N_H = number of H atoms in the periphery of a PAH molecule.

The full table of the band positions and intensities of the modes for all the possible forms is available as supplementary material to the online version of this paper.

3.1 Perylene

The intensity of the 3.3 μm feature decreases with the consecutive dehydrogenation similar to coronene. The C–C stretch modes in the 5–10 μm region are present in the spectra of dehydrogenated perylene anions as can be seen from Figs 3(a)–(f). While this is expected for all forms of ionized PAHs, a unique features at ∼5.8 is observed for dehydrogenated forms of perylene. This is analogous to the 5.2 μm band observed for a dehydrogenated coronene anion. When H atoms are removed from a perylene molecule successively, at a certain instance, one of the benzene rings in the network (appar-

ently C–C–C) are completely free of H or any other atoms. Due to the stretching of that free C–C–C bond in dehydrogenated perylene, a feature at ∼5.8 μm arises. The wavelengths beyond 10 μm are assigned to the C–H oop and C–C–C oop modes, while features beyond 20 μm arise due to the C–C–C in-plane modes.

3.2 Ovalene

Figs 3 (g)–(l) show spectra of various forms of the dehydrogenated ovalene anion. With increasing dehydrogenation, the intensity of the 3.3 μm band decreases. Apart from the other usual features that are common to all PAHs, dehydrogenated ovalene anions show a 5.2 μm band due to a free C–C bond stretch. This is similar to the 5.2 μm feature observed for a dehydrogenated coronene and does not appear for a low degree of dehydrogenation. Another

Table 2. Spectral lines in the 5–30 μm region for $C_{20}H_6^-$, $C_{24}H_6^-$ and $C_{32}H_7^-$.

$C_{20}H_6^-$		$C_{24}H_6^-$		$C_{32}H_7^-$			
λ (μm)	Int$_{rel}$	λ (μm)	Int$_{rel}$	λ (μm)	Int$_{rel}$	λ (μm)	Int$_{rel}$
5.9	1	5.1	0.21	5	0.56	9.1	0.12
6.3	0.07	5.2	1	5.1	0.96	9.3	0.17
6.3	0.19	6.9	0.28	5.2	1	9.5	0.11
6.4	0.60	7.1	0.07	6.2	0.05	9.7	0.09
6.7	0.06	7.3	0.21	6.3	0.22	10.1	0.23
7.2	0.18	7.5	0.08	6.3	0.1	11.6	0.05
7.2	0.11	8	0.09	6.5	0.19	11.6	0.08
7.4	0.21	8	0.05	6.6	0.46	11.9	0.6
7.5	0.3	9.1	0.11	6.7	0.05	12.3	0.16
7.5	0.14	9.4	0.13	6.8	0.09	12.3	0.06
7.9	0.10	10.1	0.05	6.8	0.75	12.8	0.15
8.5	0.17	10.7	0.07	6.9	0.24	13.3	0.05
8.7	0.14	12.2	0.22	6.9	0.73	13.3	0.08
8.9	0.21	12.6	0.06	7.1	0.25	14.5	0.16
9.9	0.28	12.7	0.05	7.1	0.16	14.6	0.1
9.9	0.06	16.3	0.09	7.3	0.12	14.6	0.06
12.4	0.08	19.5	0.06	7.3	0.13	15.1	0.31
12.5	0.25	20.1	0.05	7.7	0.13	16.7	0.3
13.2	0.35	22.1	0.09	7.8	0.1	16.9	0.1
16.6	0.09	23.4	0.28	7.8	0.05	17.1	0.07
26.9	0.09	26.8	0.06	7.9	0.07	18.2	0.2
28.4	0.08	30.3	0.08	8.2	0.07	19.9	0.09
				8.2	0.82	20.3	0.05
				8.4	0.24	22.6	0.21
				8.5	0.07	22.7	0.54
				8.7	0.05	24.1	0.09
				8.9	0.21	24.4	0.09
				8.9	0.07	25.0	0.46
						26.0	0.19

The full table of the band positions and intensities of the spectral lines for all the molecules is available as supplementary material to the online version of this paper.

crucial aspect is the increasing number of features with increasing size. Partial dehydrogenation of a comparatively large PAH anion ($C_{32}H_{14}^-$) shows more features distributed throughout the 5–30 μm region compared to smaller dehydrogenated PAH anions. Table 2 lists the wavelengths together with Int$_{rel}$ values that are present in a partially dehydrogenated (50 per cent dehydrogenation) perylene anion ($C_{20}H_6^-$), coronene anion ($C_{24}H_6^-$) and ovalene anion ($C_{32}H_7^-$) that shows the enhancement of features in number with size.

4 ASTROPHYSICAL IMPLICATIONS

Recent studies by Bauschlicher et al. (2008, 2009) conclude that PAH neutrals, cations and anions are equally important for some of the observed AIBs, if not all. Particularly, the 3.3 μm feature is attributed to arise from the C–H stretch mode in a neutral PAH whereas the 6.2, 7.7 and 8.6 μm features are inherent to C–C stretch/C–H in-plane modes in a PAH cation (Pech, Joblin & Boissel 2002). The 11.2 and 12.7 μm features have been attributed to the oop bending modes associated with solo and duo/trio C–H groups respectively in a neutral PAH (Hudgins & Allamandola 1999). In general, PAH cations are proposed to be promising candidates of AIB carriers in terms of intensities, while neutral PAHs are consistent with the band profiles and peak positions of the bands (Pech et al. 2002, and references therein). The ionization (positive/negative) will result in a slight blueshifting of the peak position with a distinct variation in the intensity.

Anionic PAHs have been considered to be the principal carriers of negative charge in diffuse and dense interstellar clouds (Bakes & Tielens 1998; Tielens 2008; Wakelam & Herbst 2008; Carelli & Gianturco 2012). Similar to cations, PAH anions may also contribute to the astronomical bands at 7.8 and 8.6 μm (Bauschlicher et al. 2008, 2009). The variation in the intensity of the IR bands is a function of the physical condition of the environment and can be used to probe the abundance of PAH cations/anions in the sources. Our results suggest that PAH anions show spectral characteristics that are in-between PAH neutrals and PAH cations. We also include dehydrogenated forms of PAH anions to understand any possible contribution towards the observed AIBs. PAH anions are formed through radiative attachment of electrons in dense cloud. There is a possible channel for stabilization of PAH anion by releasing an H atom to form dehydrogenated PAH anion (Sebastianelli & Gianturco 2012; Garcia-Sanz et al. 2013). The higher electron affinity of dehydrogenated PAH molecules in comparison to the parent hydrocarbon also indicates the possibility of formation of dehydrogenated PAH anions in the ISM. Le Page, Snow & Bierbaum (2001, 2003) reported that intermediate size PAHs (carbon atoms ∼ 20–30) are prone to extreme dehydrogenation, while small PAHs (fewer than 20 carbon atoms) are destroyed and large PAHs (more than 30 carbon atoms) are mostly hydrogenated/fully hydrogenated under interstellar conditions. Those with dehydrogenation can further be altered into a dehydrogenated PAH anion in dense clouds. Similar to neutral PAHs, anionic PAHs also show a distinct 3.3 μm band with a comparatively stronger intensity.

From this report, Int$_{3.3}$[5] for neutral coronene ($C_{24}H_{12}$) is 0.44 and for anionic coronene ($C_{24}H_{12}^-$), it is 0.59. Int$_{3.3}$ is large compared to the observations. Tielens (2008) pointed out that neutral PAHs can still be considered as potential candidates for the 3.3 μm band as long as the relative strength of the C–H versus the C–C modes is comparable to observations. However for the anions, Int$_{3.3}$ is so large that it only becomes comparable to observations when H atoms are removed from the periphery of the molecule. Dehydrogenation may not necessarily result into an immediate decrease in Int$_{3.3}$ as the intensity is also governed by the symmetry of the molecule. PAHs with higher symmetry show a lower value of Int$_{3.3}$ compared to less symmetric structures. As dehydrogenation proceeds, we expect to see a fall in Int$_{3.3}$ and after a certain instance, it may give an Int$_{3.3}$ which is equivalent to that of neutral and gradually may approach the Int$_{3.3}$ value obtained for a PAH cation. For example, $C_{24}H_8^-$ has Int$_{3.3}$ ∼ 0.37 which is then close to the value obtained for $C_{24}H_{12}$. Thus, $C_{24}H_8^-$ may be equally important as $C_{24}H_{12}$ for the astronomically observed feature at 3.3 μm. The low symmetry structures of dehydrogenated coronene containing an odd number of H atoms usually show a higher value of Int$_{3.3}$ compared to high symmetric structures with an even number of H atoms as shown in Table 3. $C_{24}H_2^-$ gives Int$_{3.3}$ ∼ 0.07 which is close to the Int$_{3.3}$ ∼ 0.02 obtained for $C_{24}H_{12}$ cation. Perylene ($C_{20}H_{12}$) also shows similar behaviour and on partial dehydrogenation, $C_{20}H_{10}^-$ gives Int$_{3.3}$ ∼ 0.59 which is close to the Int$_{3.3}$ obtained for $C_{20}H_{12}$ (Int$_{3.3}$ ∼ 0.69). Int$_{3.3}$ for the $C_{20}H_{12}$ anion is high (∼0.93). Increasing dehydrogenation will give even a lower value of Int$_{3.3}$ as discussed for coronene. As for ovalene ($C_{32}H_{14}$), the situation is somewhat different and Int$_{3.3}$ obtained for its neutral, anionic and cationic forms are 0.83, 0.29, 0.07, respectively. Int$_{3.3}$ increases to 1 when we remove the first H atom from $C_{32}H_{14}^-$ (i.e. for $C_{32}H_{13}^-$) and it then comes down to a lower

---

[5] The highest C–H$_{stretch}$ intensity among all the C–H$_{stretch}$ vibrations is considered.

Table 3. Int$_{3.3}$ obtained for dehydrogenated forms of coronene anion.

Dehydrogenated coronene anion	Int$_{3.3}$
$C_{24}H_{11}^-$	0.63
$C_{24}H_{10}^-$	0.92
$C_{24}H_9^-$	0.99
$C_{24}H_8^-$	0.37
$C_{24}H_7^-$	1
$C_{24}H_6^-$	0.16
$C_{24}H_5^-$	0.72
$C_{24}H_4^-$	0.21
$C_{24}H_3^-$	1
$C_{24}H_2^-$	0.07
$C_{24}H_1^-$	0.45

value for a $C_{32}H_{10}^-$ (Int$_{3.3} \sim 0.37$), $C_{32}H_6^-$ (Int$_{3.3} \sim 0.32$) and so on. For $C_{32}H_3^-$ and $C_{32}H_1^-$, Int$_{3.3}$ is 0.08 and 0.06 respectively which are comparable to observations.

Dehydrogenation also results in the rise of features in the 5–10 μm region. The same characteristic is also observed for cationic PAH molecules. A band at 5.2 μm is a unique feature present only in strongly dehydrogenated PAH anions. This feature may help in identification of dehydrogenated PAH anions in the ISM. Its absence also suggests that the size of PAHs studied here may be only weakly dehydrogenated. Another important characteristic is that with increasing dehydrogenation, a broad plateau in the 20–30 μm region gains intensity mainly due to C–C–C in-plane modes. With increasing size, this feature gains intensity. This region together with the other characteristics mentioned here may be used as a probe to identify any possible dehydrogenated forms of PAH anions in the ISM. [FePAH]$^+$ complexes also show intense features in the 20–60 μm regions (Simon & Joblin 2010), however the assignment of carriers in the far-infrared region is still ambiguous. This calls for new astronomical data in the far-infrared which would help concretize theoretical results.

It is important to note here that interstellar PAHs usually exist either in fully hydrogenated or in fully dehydrogenated form and the intermediate hydrogenated/dehydrogenated state is rare (Mackie et al. 2015). Le Page et al. (2001, 2003) suggest that partial dehydrogenation may be possible for intermediate size PAHs (carbon atoms ∼20–30). In such a scenario, intermediate dehydrogenation states for $C_{32}H_{14}$ may exist long enough to emit the AIBs. Once all the H atoms are removed, a C atom may be lost subsequently to form a pentagonal ring which will then initiate the formation of fullerenes in the ISM (Mackie et al. 2015). Dehydrogenation may therefore be considered as an intermediate phase in the formation of a fullerene from a PAH molecule.

5 SUMMARY

Interstellar PAH anions are likely to exist in cold dense regions where a PAH molecule can easily attract an electron to form a PAH anion that shows important characteristic features in IR. This study reports the vibrational study of dehydrogenated PAH anions to seek any correlation with the observed AIBs. The theoretical data show that PAH anions along with their dehydrogenated forms show characteristics that are similar to neutrals and cations. This implies that the astronomically observed bands that are usually assigned to either a neutral or a cationic PAH are also likely to have contributions from dehydrogenated PAH anions provided that the physical conditions support their presence in the ISM.

We summarize the results here:

1. Partially dehydrogenated PAH anions may contribute to the 3.3 μm region and the broad intense features in the 5–10 μm region.

2. The 3.3 μm feature is immensely strong for a PAH anion. Dehydrogenation of a PAH anion reduces the intensity of the 3.3 μm feature which then becomes comparable to its neutral counterpart and is closer to observed intensities of regions where the 3.3 μm is intense.

3. During the process of successive dehydrogenation, the molecule passes through a series of changes in its symmetry. The dehydrogenated PAH anion with a higher symmetry produces a less intense 3.3 μm band than that with a lower symmetry.

4. During the process of dehydrogenation, a duo C–H group in the PAH anion may convert into a solo C–H unit which produces a 3.4 μm feature due to the solo C–H stretch vibrations.

5. Unique features at 5.2 and 5.8 μm are observed for a dehydrogenated PAH anion that arise due to the stretching of the free C–C/C–C–C stretch. The 5.2 μm band observed in coronene and ovalene may be used to identify dehydrogenated PAH anions. Absence of this feature in observations suggests that such PAHs may be dehydrogenated up to a certain limit.

6. A broad plateau in the 20–30 μm region arises in the spectra of a dehydrogenated PAH anion that becomes more significant with increasing size.

These characteristics can be used as a tool to understand any possible contribution of dehydrogenated PAH anions in the ISM. The calculated energy configuration indicates that before they convert into fully dehydrogenated molecules, a partially dehydrogenated form of PAH anion may be present for a large PAH molecule as it is less susceptible to the loss of H atoms and requires time to remove all the H atoms from its periphery. The spectral characteristics together with stability offers support to the existence of large dehydrogenated PAH anions in the ISM as members of the extended PAH family.

REFERENCES

Acke B., van den Ancker M. E., 2004, A&A, 426, 151
Allamandola L. J., Tielens A. G. G. M., Barker J. R., 1985, ApJ, 290, L25
Allamandola L. J., Tielens A. G. G. M., Barker J. R., 1989, ApJS, 71, 733
Armus L. et al., 2007, ApJ, 656, 148
Bakes E. L. O., Tielens A. G. G. M., 1994, ApJ, 427, 822
Bakes E. L. O., Tielens A. G. G. M., 1998, ApJ, 499, 258
Bakes E. L. O., Tielens A. G. G. M., Bauschlicher C. W., Jr, 2001a, ApJ, 556, 501

Bakes E. L. O., Tielens A. G. G. M., Bauschlicher, Jr C. W., Hudgins D. M., Allamandola L. J., 2001b, ApJ, 560, 261

Bauschlicher C. W., Jr, Peeters E., Allamandola L. J., 2008, ApJ, 678, 316

Bauschlicher C. W., Jr, Peeters E., Allamandola L. J., 2009, ApJ, 697, 311

Bauschlicher C. W., Ricca A., Jr, 2013, ApJ, 776, 102

Berné O., Tielens A. G. G. M., 2012, Proc. Natl. Acad. Sci. USA, 109, 401

Brandl B. R. et al., 2006, ApJ, 653, 1129

Buragohain M., Pathak A., Sarre P., Onaka T., Sakon I., 2015, MNRAS, 454, 193

Buragohain M., Pathak A., Sarre P., Onaka T., Sakon I., 2016, Planet. Space Sci., 133, 97

Campbell E. K., Holz M., Gerlich D., Maier J. P., 2015, Nature, 523, 322

Candian A., Sarre P. J., Tielens A. G. G. M., 2014, ApJ, 791, L10

Carelli F., Gianturco F. A., 2012, MNRAS, 422, 3643

Cox N. L. J., Cordiner M. A., Cami J., Foing B. H., Sarre P. J., Kaper L., Ehrenfreund P., 2006, A&A, 447, 991

DeFrees D. J., Miller M. D., Talbi D., Pauzat F., Ellinger Y., 1993, ApJ, 408, 530

Duley W. W., Williams D. A., 1981, MNRAS, 196, 269

Dunk P. W. et al., 2012, Nat. Commun., 3, 855

Ehrenfreund P., Foing B., 2015, Nature, 523, 296

Fortenberry R. C., Moore M. M., Lee T. J., 2016, J. Phys. Chem. A, 120, 7327

Garcia-Sanz A., Carelli F., Sebastianelli F., Gianturco F. A., Garcia G., 2013, New J. Phys., 15, 013018

Hammonds M., Pathak A., Candian A., Sarre P. J., 2011, in Joblin C., Tielens A. G. G. M., eds, PAHs and the Universe: A Symposium to Celebrate the 25th Anniversary of the PAH Hypothesis, EAS Publ. Ser., Toulouse, France, Vol. 46. p. 373

Herbst E., 1981, Nature, 289, 656

Herbst E., Osamura Y., 2008, ApJ, 679, 1670

Hony S., Van Kerckhoven C., Peeters E., Tielens A. G. G. M., Hudgins D. M., Allamandola L. J., 2001, A&A, 370, 1030

Hudgins D. M., Allamandola L. J., 1999, ApJ, 516, L41

Hudgins D. M., Bauschlicher C. W., Jr, Sandford S. A., 2004, ApJ, 614, 770

Hudgins D. M., Bauschlicher C. W., Jr, Allamandola L. J., 2005, ApJ, 632, 316

Langhoff S. R., 1996, J. Phys. Chem., 100, 2819

Le Page V., Snow T. P., Bierbaum V. M., 2001, ApJS, 132, 233

Le Page V., Snow T. P., Bierbaum V. M., 2003, ApJ, 584, 316

Léger A., Puget J. L., 1984, A&A, 137, L5

Lepp S., Dalgarno A., 1988a, ApJ, 335, 769

Lepp S., Dalgarno A., 1988b, ApJ, 324, 553

Mackie C. J., Peeters E., Bauschlicher C. W., Jr, Cami J., 2015, ApJ, 799, 131

Malloci G., Mulas G., Cappellini G., Fiorentini V., Porceddu I., 2005, A&A, 432, 585

Malloci G., Joblin C., Mulas G., 2007, A&A, 462, 627

McCarthy M. C., Gottlieb C. A., Gupta H., Thaddeus P., 2006, ApJ, 652, L141

Omont A., 1986, A&A, 164, 159

Onaka T., Yamamura I., Tanabe T., Roellig T. L., Yuen L., 1996, PASJ, 48, L59

Onaka T., Mori T. I., Sakon I., Ohsawa R., Kaneda H., Okada Y., Tanaka M., 2014, ApJ, 780, 114

Pathak A., Rastogi S., 2005, Chem. Phys., 313, 133

Pathak A., Rastogi S., 2006, Chem. Phys., 326, 315

Pathak A., Rastogi S., 2007, Spectrochim. Acta A, 67, 898

Pathak A., Sarre P. J., 2008, MNRAS, 391, L10

Pauzat F., 2011, in Joblin C., Tielens A. G. G. M., eds, PAHs and the Universe: A Symposium to Celebrate the 25th Anniversary of the PAH Hypothesis, EAS Publ. Ser., Toulouse, France Vol. 46. p. 75

Pauzat F., Talbi D., Ellinger Y., 1997, A&A, 319, 318

Pauzat F., Lattelais M., Ellinger Y., Minot C., 2011, MNRAS, 412, 2729

Pech C., Joblin C., Boissel P., 2002, A&A, 388, 639

Peeters E., Hony S., Van Kerckhoven C., Tielens A. G. G. M., Allamandola L. J., Hudgins D. M., Bauschlicher C. W., 2002, A&A, 390, 1089

Peeters E., Allamandola L. J., Bauschlicher C. W., Jr, Hudgins D. M., Sandford S. A., Tielens A. G. G. M., 2004, ApJ, 604, 252

Regan M. W. et al., 2004, ApJS, 154, 204

Ruiterkamp R., Halasinski T., Salama F., Foing B. H., Allamandola L. J., Schmidt W., Ehrenfreund P., 2002, A&A, 390, 1153

Sakon I., Onaka T., Ishihara D., Ootsubo T., Yamamura I., Tanabé T., Roellig T. L., 2004, ApJ, 609, 203

Salama F., Galazutdinov G. A., Krełowski J., Biennier L., Beletsky Y., Song I.-O., 2011, ApJ, 728, 154

Sarre P. J., 2006, J. Mol. Spectrosc., 238, 1

Schmidt T. W., Pino T., Bréchignac P., 2009, J. Phys. Chem. A, 113, 3535

Sebastianelli F., Gianturco F. A., 2012, Eur. Phys. J. D, 66, 41

Shao Y. et al., 2015, Mol. Phys., 113, 184

Simon A., Joblin C., 2010, ApJ, 712, 69

Simon A., Rapacioli M., Lanza M., Joalland B., Spiegelman F., 2011, Phys. Chem. Chem. Phys., 13, 3359

Snow T. P., Le Page V., Keheyan Y., Bierbaum V. M., 1998, Nature, 391, 259

Szczepanski J., Wehlburg C., Vala M., 1995, Chem. Phys. Lett., 232, 221

Theis M. L., Candian A., Tielens A. G. G. M., Lee T. J., Fortenberry R. C., 2015, J. Phys. Chem. A, 119, 13048

Tielens A. G. G. M., 2008, ARA&A, 46, 289

Tobita S., Meinke M., Illenberger E., Christophorou L. G., Baumgärtel H., Leach S., 1992, Chem. Phys., 161, 501

Verstraete L., Léger A., d'Hendecourt L., Defourneau D., Dutuit O., 1990, A&A, 237, 436

Verstraete L., Puget J. L., Falgarone E., Drapatz S., Wright C. M., Timmermann R., 1996, A&A, 315, L337

Wakelam V., Herbst E., 2008, ApJ, 680, 371

Wang H., Szczepanski J., Hirata S., Vala M., 2005, J. Phys. Chem. A, 109, 9737

Yang X., Glaser R., Li A., Zhong J., 2017a, New Astron. Rev., 77, 1

Yang X. J., Li A., Glaser R., Zhong J. X., 2017b, ApJ, 837, 171

SUPPORTING INFORMATION

Supplementary data are available at *MNRAS* online.

supplementary_dehydrogenated_anion.txt

Please note: Oxford University Press is not responsible for the content or functionality of any supporting materials supplied by the authors. Any queries (other than missing material) should be directed to the corresponding author for the article.

This paper has been typeset from a TEX/LATEX file prepared by the author.